JTTEE5 4:185-194

Vacuum Plasma Spraying of High-Performance Electrodes for Alkaline Water Electrolysis

G. Schiller, R. Henne, and V. Borck

Electrode coatings for advanced alkaline water electrolysis were produced by applying the vacuum plasma spraying (VPS) process. The characteristics of the used VPS equipment that were essential for the development of effective electrocatalytic electrode layers are presented. Molybdenum-containing Raney nickel coatings were applied for cathodic hydrogen evolution, and Raney nickel/Co_3O_4 matrix composite layers were developed for the anodic oxygen evolution reaction. For the preparation of Raney nickel coatings, a precursor alloy such as Ni-Al was sprayed that had to be leached subsequently in caustic solution to remove the aluminum content, forming a porous, high-surface-area nickel layer. The spray powders and the resulting VPS layers were studied by metallography, x-ray diffraction (XRD), and scanning electron microscopy/energy dispersive analysis by x-ray (SEM/EDX). For spraying of thermally sensitive oxide electrocatalysts (e.g., Co_3O_4), special process conditions involving plasma-chemical effects (reactive plasma spraying) had to be developed. The electrocatalytic activity of the electrode coatings was investigated by performing polarization curves free of ohmic losses (IR-free) and long-term tests under conditions of continuous and intermittent operation, which showed excellent electrochemical properties.

1. Introduction

RENEWABLE energies may be a substantial part of the energy used in the future, simultaneously avoiding any increase in environmental pollution and moderating the CO_2 problem. But since nonfossil and nonnuclear primary energies such as solar irradiation or wind energy are only intermittently available, it is necessary to convert them into a secondary energy carrier that is storable and transportable.

Hydrogen produced by water electrolysis represents the most attractive energy carrier to meet these requirements (Ref 1). For effective and economical hydrogen production, advanced electrolyzers with high-performance electrodes that are also suited for intermittent operation have to be developed. Using electrocatalytically highly active coatings on electrodes, the energy efficiency of water electrolysis can be improved.

Raney nickel is one of the catalytically most active materials and is used for both cathodes and anodes in alkaline water electrolysis (Ref 2-4). The outstanding electrochemical properties of this material arise mainly from its large effective surface area, which results from its high porosity and nanocrystalline structure. Raney nickel is produced by leaching the aluminum content of a precursor alloy (Ni-Al) with caustic solution, leaving a porous, high-surface-area nickel residue. The enhancement of the surface area compared to the geometric electrode surface area leads to lower local current densities and thus to the reduction of overvoltage.

For cathodic hydrogen evolution, some indications can be found in the literature about the beneficial effect of adding molybdenum to Raney nickel (Ref 5, 6) to improve its catalytic efficiency as well as its long-term stability. For anodic oxygen evolution, mixed oxides of nonnoble metals, for instance cobalt-containing spinels and perovskites, have good catalytic activity (Ref 7, 8). Combining the high specific surface area and the good electrical conductivity of Raney nickel with the catalytic activity of these oxide electrocatalysts should result in improved anodes.

Conventional preparation methods for electrode coatings, such as sinter process, thermal decomposition of salts, or galvanic deposition, exhibit considerable disadvantages. With thermal decomposition and sinter processes, undesired decomposition or phase transformations may occur at the high temperatures and long reaction times. Only thin layers can be achieved by this one process step, and the resulting layers may have low mechanical stability. The process temperatures are usually far below the melting points of the materials; thus, process times are relatively long, and thick layers with definite and variable structures in terms of porosity or composition are difficult to produce. Galvanic deposition is restricted to few metals and alloys, and there are environmental problems of galvanic waste water clarification associated with this process.

At the German Aerospace Research Establishment (DLR) in Stuttgart, vacuum plasma spraying (VPS) has been developed and adapted to meet the requirements for the production of electrochemical components (Ref 9-11). The modified VPS technique has proved to be an effective method to produce both Raney nickel (Mo) cathode coatings and Raney nickel/Co_3O_4 matrix anode coatings that show high electrochemical performance in alkaline water electrolysis.

Keywords: cobalt oxide feedstock, feedstock phase changes, oxide electrocatalyst, Raney nickel coatings, vacuum plasma spraying, water electrolysis

G. Schiller, R. Henne, and **V. Borck,** Deutsche Forschungsanstalt für Luft- und Raumfahrt (DLR), Institute of Technical Thermodynamics, Pfaffenwaldring 38-40, 70569 Stuttgart, Germany.

2. Experimental Procedure

2.1 *VPS Equipment*

The equipment used at DLR Stuttgart (Fig. 1) is based on commercially available components (Plasmatechnik AG, Wohlen, Switzerland), but essential parts have been developed in-house to adapt the spray process to requirements of electrode layers to

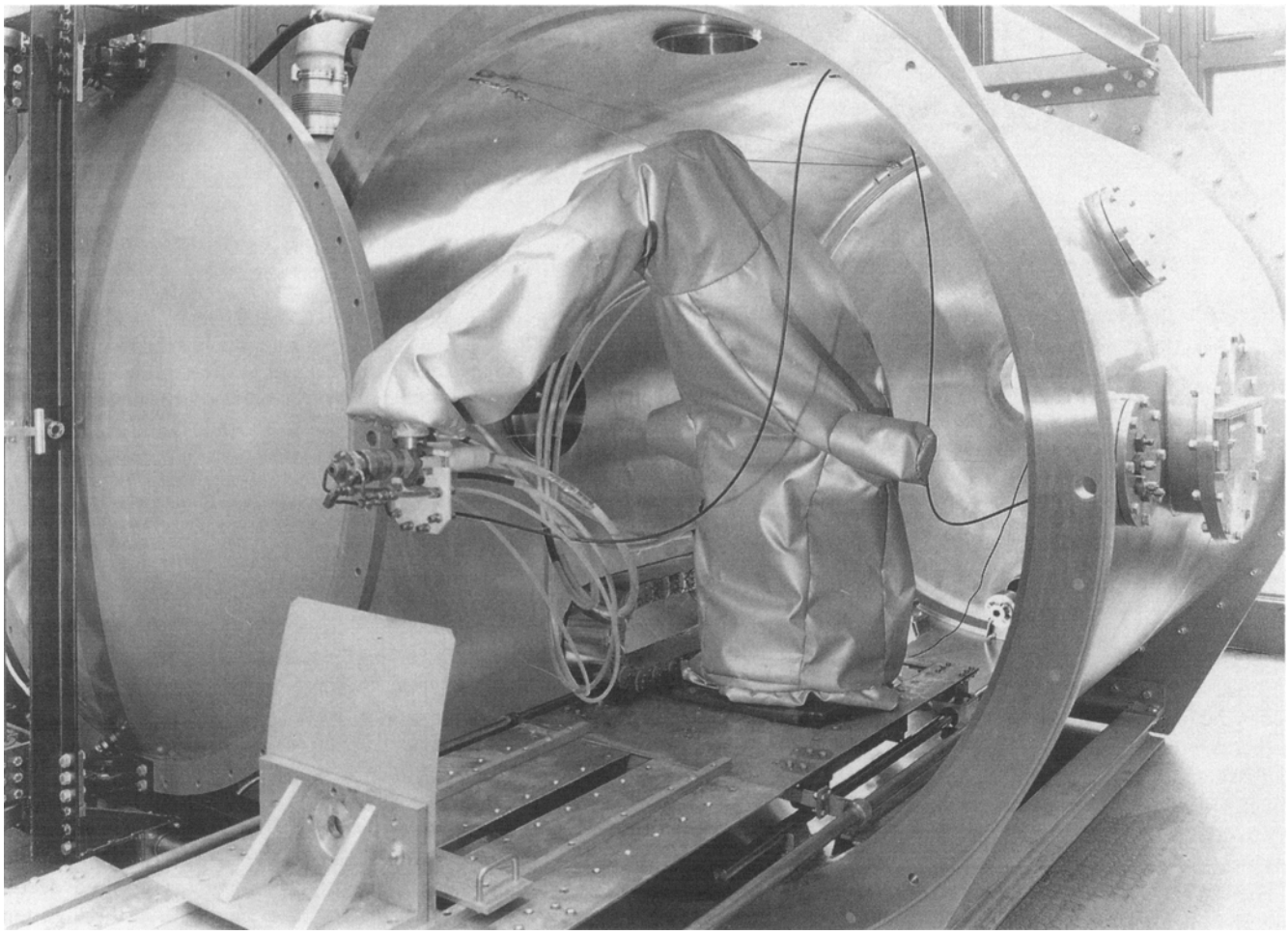

Fig. 1 VPS equipment at DLR Stuttgart. The chamber diameter is 1.7 m and the length is 2.2 m.

be produced for electrochemical applications. The modifications are related especially to the plasma torch and the nozzle (Fig. 2). In order to generate a long and laminar plasma jet, nozzles with Laval-like contours designed for supersonic velocities (Mach 2 to Mach 5) have been developed and investigated by analytical methods (Ref 12, 13). Laval nozzles have been added to a standard APS (atmospheric plasma spraying) torch (PT-F4) so that plasma jet velocities of up to 3000 m/s can be reached, which accelerate the powder particles to in excess of 800 m/s. Laser doppler anemometry measurements reveal that the spray material passes close and parallel to the jet axis, resulting in favorable melting conditions and good protection of the spray material against disadvantageous interactions with surrounding gases. Owing to the long homogeneous plasma jet and the well-concentrated spray material close to the jet axis, the powder is completely melted despite the very short dwell time of less than 1 ms within the plasma. Recently, novel plasma torches have been developed in which the "Laval" nozzle contour is integrated within the anode of the plasma torch (Ref 14).

Another feature of the used plasma torches is the internal powder injection by several integrated powder injection ports, which are arranged at different positions along the Laval nozzle. This arrangement allows the spraying of very different materials, depending on the requirements of the powders to be sprayed. One injection area is located close to the nozzle notch where the plasma is relatively dense, hot, and slow. High energy exchange between plasma and particles enhances favorable melting conditions for powders with a high melting temperature, which are preferably fed at this location. Powders with lower melting points can be injected close to the nozzle mouth at the end of the nozzle to avoid overheating of the particles. By optimization of the spray parameters and utilization of the different powder injection ports, complex coatings exhibiting a desired material and porosity profile, such as matrix composite layers consisting of metallic and oxide components, can be realized.

The powder injection ports of the torch can also be used for feeding additional gases into the plasma. If this takes place very close to the plasma-generating zone, these gases will be ionized and activated, resulting in plasma-chemical effects. The processing of thermally sensitive oxide electrocatalysts by VPS, as described below for the production of composite anode coatings, is essentially based on the development of this "reactive plasma spraying" process.

2.2 *Spray Powders*

Nickel-aluminum precursor alloy powder is vacuum plasma sprayed for the preparation of Raney nickel layers. In a sub-

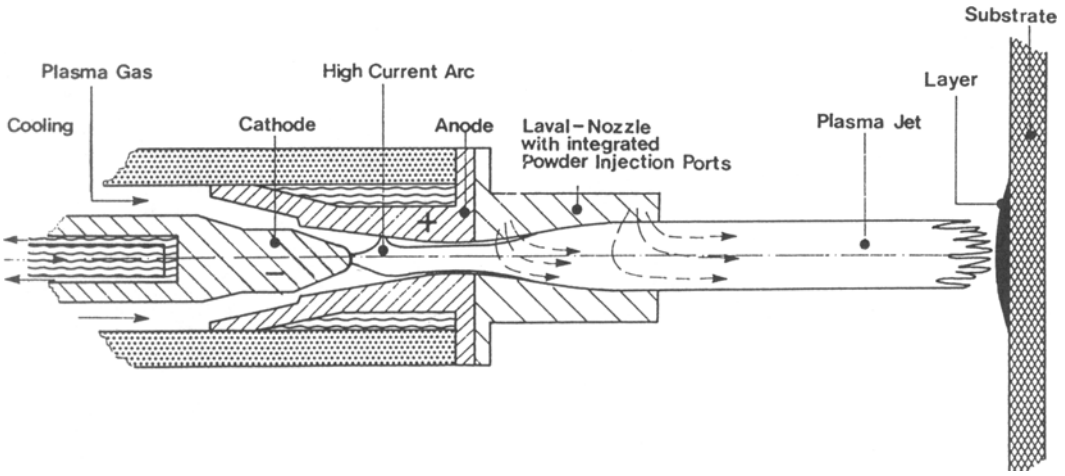

Fig. 2 Principle of the DLR VPS torch with Laval nozzle

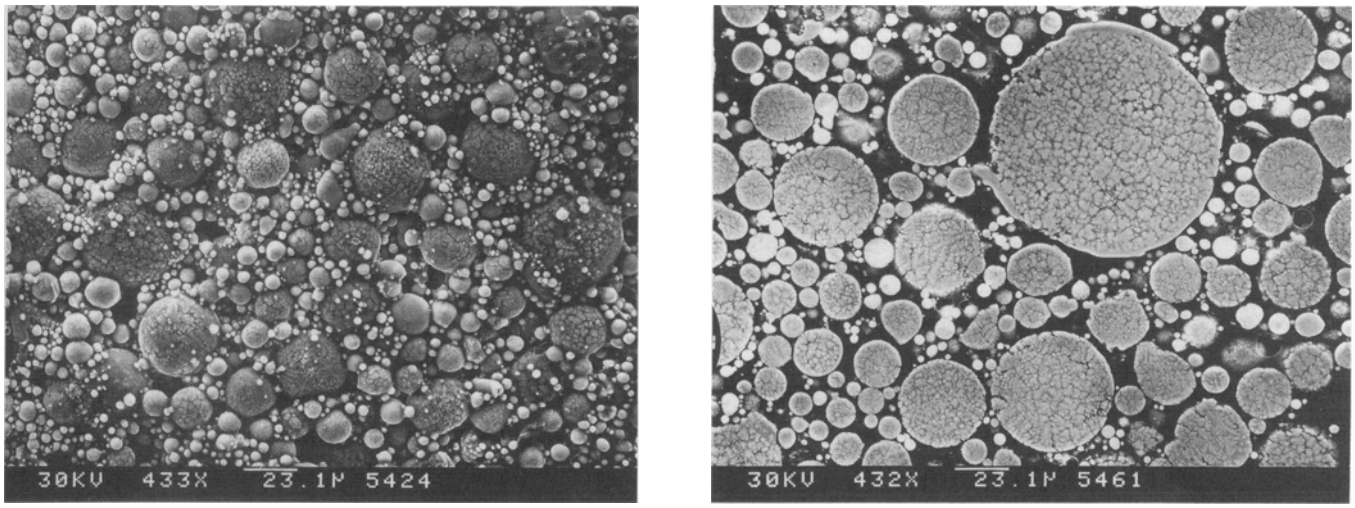

(a) **(b)**

Fig. 3 Micrographs of NiAl50 powder. (a) Morphology. (b) Cross section

sequent activation process, the aluminum content is leached in KOH solution, forming a structured, high-surface-area Raney nickel layer. In order to improve the catalytic properties of the cathode coatings, molybdenum is added to the Ni-Al precursor alloy, either by mixing the components prior to spraying or by alloying to prepare a ternary Ni-Al-Mo alloy. Mixtures of Ni-Al alloy and Co_3O_4 spinel serve as spray powders to produce matrix composite layers for the anodes.

2.2.1 Ni-Al/Mo Mixture and Ni-Al-Mo Alloy

Gas-atomized NiAl50 (H.C. Starck, Germany) and molybdenum powder (E. Merck, Darmstadt, Germany) were used to prepare the Ni-Al/Mo mixture. The multiphase NiAl50 powder (50 wt% Ni, 50 wt% Al) with a particle size fraction below 180 μm, consists predominantly of the phases Ni_2Al_3 and $NiAl_3$ (Fig. 3). The cross section of the gas-atomized NiAl50 powder (Fig. 3b) exhibits a large number of fine particles between 10 and 50 μm and some large spherical agglomerates of about 100 μm. The particles show cracks and voids, indicating a low mechanical stability of the grains. The particle size of the molybdenum powder was below 20 μm. Both powders were mixed for about 4 h. The optimum weight percentage of molybdenum with respect to the electrochemical performance was 5 wt%. The Ni-Al-Mo alloy consisted of 17 wt% Mo, 37 wt% Ni, and 46 wt% Al. A Mo-Ni key alloy was melted together with aluminum, followed by a gas atomization process in argon atmosphere. The resulting spherical particles (Fig. 4) had a size below 43 μm and were fine grained.

2.2.2 Ni-Al/Co_3O_4 Powder Mixture

The feedstock for the anode layers consisted of mixtures of the gas-atomized NiAl50 and Co_3O_4 (Cerac, Milwaukee, WI, USA). The particle size fraction of the Co_3O_4 powder is below 44 μm, with a large number of very small particles (Fig. 5).

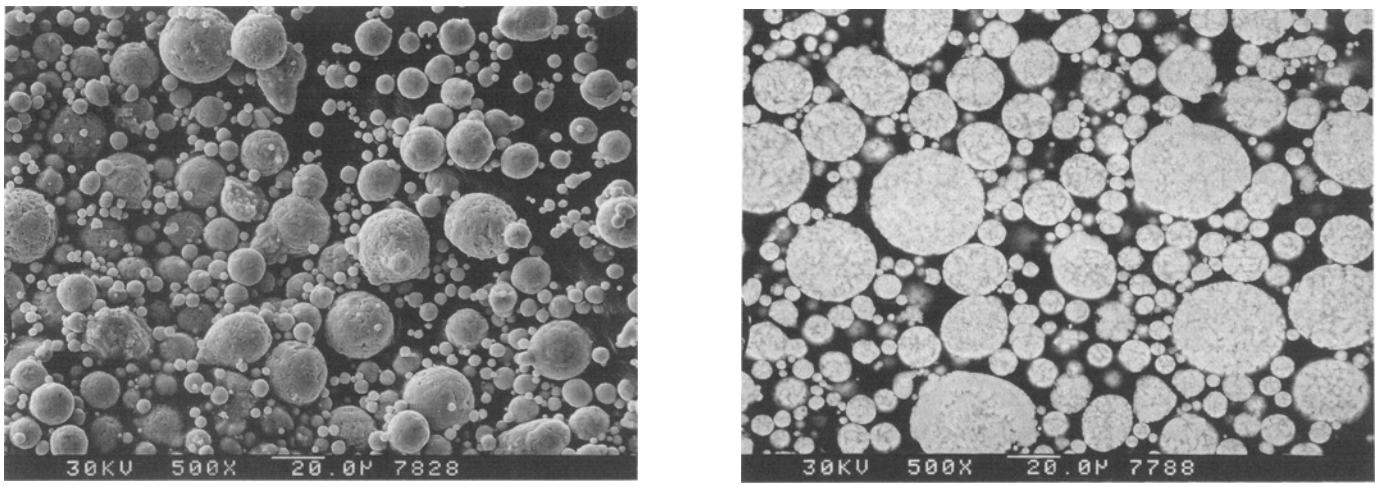

(a) (b)

Fig. 4 Micrographs of Ni-Al-Mo powder. (a) Morphology. (b) Cross section

2.3 *Activation Procedure*

The electrodes were activated in 25 wt% KOH solution at 80 °C for 24 h to form the high-surface-area Raney nickel layers. To avoid a precipitation of aluminum hydroxide in the micropores of the obtained sponge-like structure, the solution contained 10 wt% KNa tartrate-tetrahydrate as a complex former. As the resulting Raney nickel is highly pyrophoric, the electrodes had to be kept under water after activation. If analytical investigation of activated layers in air was required (SEM, XRD, metallography), a controlled oxidation in an argon-filled tank with a low concentration of oxygen had to take place to form a passivating thin oxide film on the surface.

2.4 *Electrochemical Measurements*

All electrochemical measurements were performed by means of computer-controlled electrolysis test cells with automated data acquisition and processing. Half cells with a working electrode (1 cm^2 geometric area), a nickel-plate counter electrode, and a Hg/HgO reference electrode were fixed in vessels containing 25 wt% KOH solution as the electrolyte. The temperature was kept constant at 70 °C by means of a thermostated water bath. Polarization curves in the current density range of 0.05 to 1.0 A/cm^2 were measured galvanostatically. The IR-free cathode and anode overpotentials with reference to the hydrogen (–920 mV) and oxygen equilibrium potentials (+300 mV) were determined by means of a fast current interrupter and a transient recorder.

3. Results and Discussion

3.1 *Raney Nickel (Mo) Cathodes*

The addition of molybdenum to Ni-Al improves the catalytic efficiency as well as the long-term stability of Raney nickel cathodes. There appear to be synergetic effects between nickel and molybdenum that are based on their electronic structure and that give rise to materials stabilization.

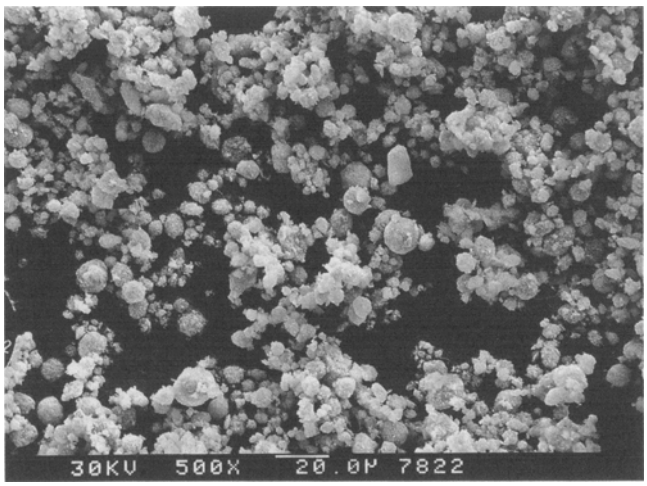

Fig. 5 Micrograph of the morphology of Co_3O_4 powder

For spraying of Ni-Al/Mo mixed powders and Ni-Al-Mo alloy powder, the same thermal spray parameters were chosen (Table 1). Spray powder quality, spray parameters, and layer consolidation conditions influence the resulting crystallographic structure, the size distribution of the microcrystals, the grain boundaries, the resulting porosity after leaching, the effective surface area, and finally the electrochemical properties of the electrodes. With increasing torch power, for example, the mechanical stability of the layer increases, but simultaneously the electrochemical quality of the layer decreases due to a reduced activation potential. Therefore, a compromise regarding all relevant parameters had to be found. At the relatively low power level, only the molybdenum particles below 20 µm could be melted sufficiently. Perforated nickel sheets of 0.35 mm thickness served as substrates. Prior to coating they were sand-

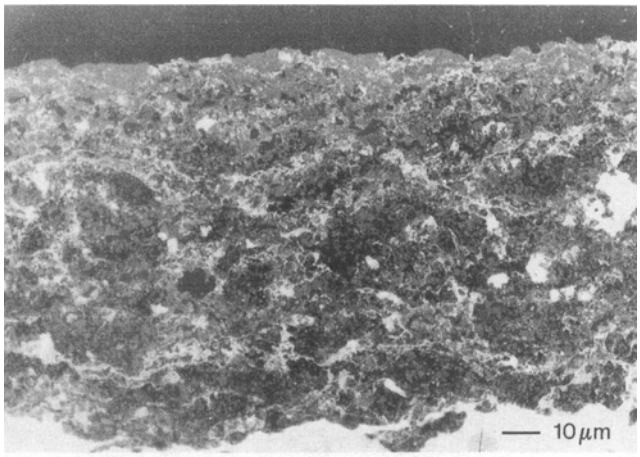

Fig. 6 Micrograph of a cross section of a VPS layer of Ni-Al/Mo powder mixture

Table 1 VPS parameters for spraying of Ni-Al/Mo mixed powder and Ni-Al-Mo alloy

Parameter	Value
Torch power	16 kW (290 A, 55 V)
Primary gas	Ar, 42 SLPM
Secondary gas	H_2, 5 SLPM
Powder feed gas	Ar, 2 SLPM
Tank pressure	30 mbar
Spraying distance	23 cm

SLPM ≡ standard liters per minute

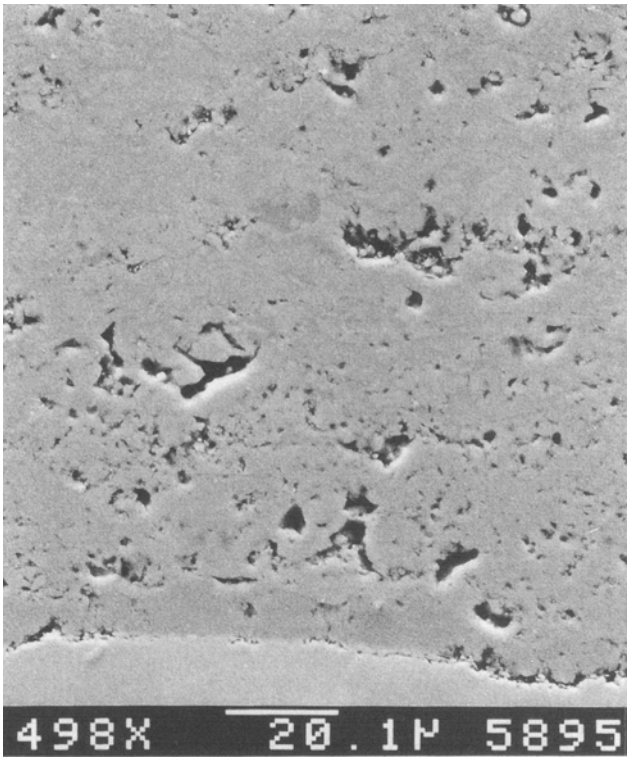

Fig. 7 Micrograph of a cross section of a VPS layer of Ni-Al-Mo alloy

Table 2 Phase composition of the as-cast Ni-Al-Mo alloy

Average of five measurements with quantitative EDX

	Composition, at.%		
Phase	Mo	Ni	Al
Ni_2Al_3	0.3	35.7	63.9
$NiAl_3$	0.2	22.9	76.9
Mo_2NiAl_5	24.0	5.1	70.9

blasted and chemically etched by 34% HCl solution. An optimum layer thickness was in the range of 100 to 150 μm.

Metallographic cross sections of VPS layers of Ni-Al/Mo powder mixture and Ni-Al-Mo alloy powder are shown in Fig. 6 and 7. The use of fine molybdenum powder for the mixed Ni-Al/Mo feedstock allowed the formation of a very homogeneous molybdenum distribution within the coating, as observed by SEM/EDX studies. Molybdenum islands with a size of 1 to 3 μm were found with a mean distance of 2 to 10 μm. The x-ray diffraction pattern of a mixed Ni-Al/Mo layer (Fig. 8a) reveals that the addition of molybdenum did not change the phase composition of the Ni-Al alloy consisting of the phases Ni_2Al_3 and $NiAl_3$; only additional peaks of pure molybdenum are observed. According to XRD and EDX analysis, alloying of Ni-Al and molybdenum was not significant during the spray process, since the temperature and diffusion time seem to be too low.

The XRD pattern of Ni-Al-Mo alloy powder is shown in Fig. 9(a). In addition to the Ni_2Al_3 phase, the pattern of an unknown phase is observed, which is assumed to be a ternary Ni-Al-Mo alloy phase even though ASTM data on such phases are lacking. The content of the phase $NiAl_3$ is very low compared to the binary gas-atomized NiAl50 powder. Quantitative SEM/EDX analysis resulted in the alloy compositions given in Table 2, which indicate three alloy phases. Apart from the Ni-Al phases of Ni_2Al_3 and $NiAl_3$, which exhibit a low solubility of molybdenum, as expected from the ternary phase diagram (Ref 15), a ternary Ni-Al-Mo phase is found with a composition close to that of phase "N" (Mo_2NiAl_5) (Ref 15-17). The growth of the Ni_2Al_3 phase at the expense of the $NiAl_3$ phase can be explained by the thermal undercooling and the high cooling rate during the gas atomization process, which favors the formation of Ni_2Al_3 due to its high formation rate and the primary solidification of the ternary phase N with high aluminum content.

The phase composition of the as-sprayed layer from the Ni-Al-Mo alloy, demonstrated by the XRD pattern in Fig. 9(b), is similar to that of the feedstock. The enrichment of the phase Ni_2Al_3 has beneficial consequences concerning layer stability, as Ni_2Al_3 results in a mechanically stronger and more active Raney nickel residue (Ref 18). In this context it is worth noticing that as-sprayed commercial Ni-Al also consists of nearly pure Ni_2Al_3 in the first 30 μm close to the substrate when sprayed on cool nickel sheets.

After activation of the electrodes in aqueous KOH solution, molybdenum-containing high-surface-area Raney nickel layers

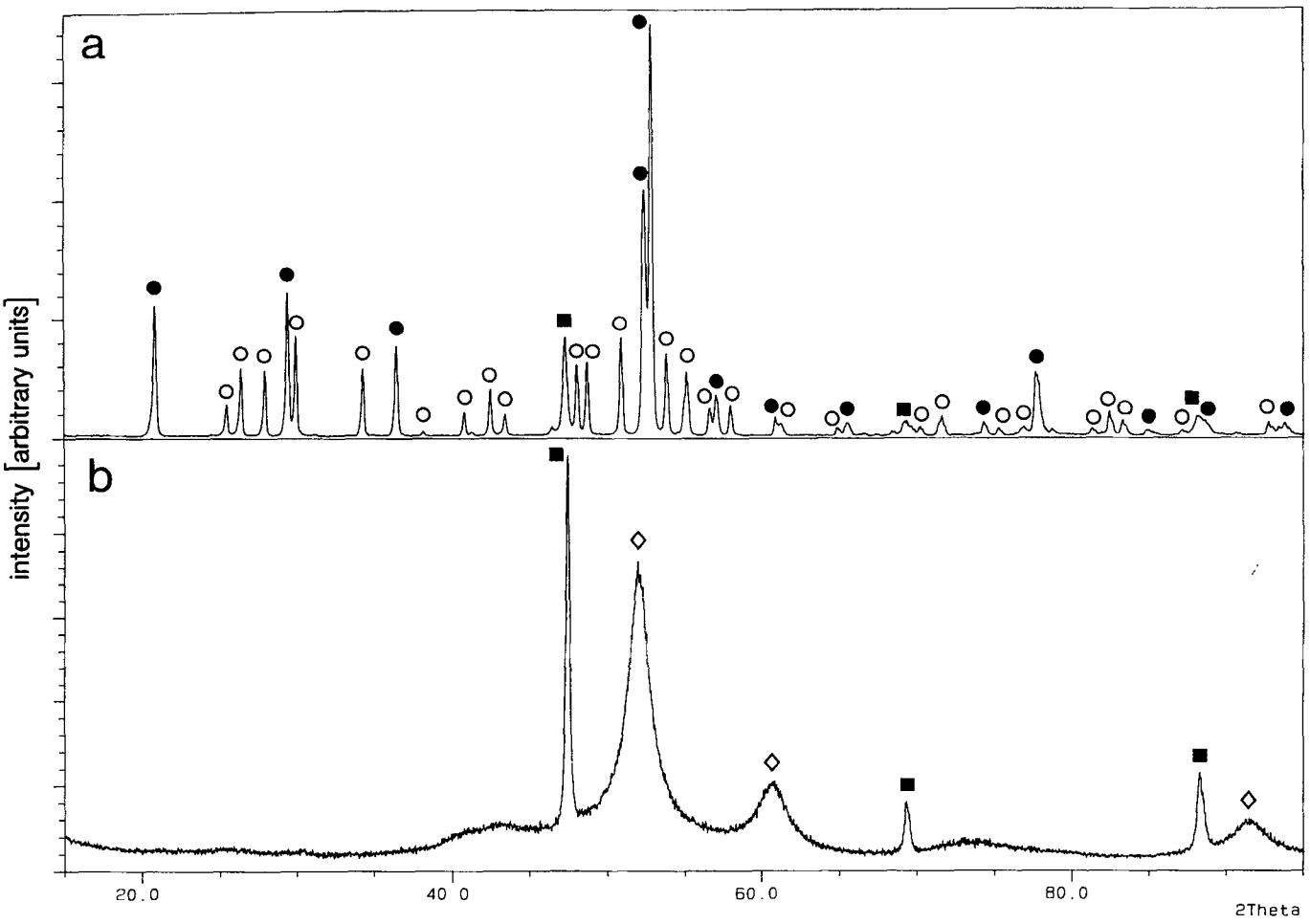

Fig. 8 XRD patterns of (a) an as-sprayed VPS layer of mixed Ni-Al/Mo and (b) the resulting activated layer. The crystallographic phases are indicated by the following symbols: ● Ni_2Al_3, ○ $NiAl_3$, ■ Mo, ◊ Ni.

form. A metallographic cross section of such an activated Raney nickel layer is shown in Fig. 10. The XRD pattern (Fig. 8b) and SEM micrographs of the activated layers originating from Ni-Al/Mo mixed powder reveal inclusions of pure molybdenum, which are coarse compared to the Raney nickel. The homogeneity of the molybdenum distribution within the activated layer compared to that of the as-sprayed coatings has further increased. The XRD pattern of an activated Ni-Al-Mo layer (Fig. 9c) shows no distinct molybdenum peaks; only very broad nickel peaks are observed. From the peak widths at half-maximum of the XRD peak profiles, mean crystallite sizes can be evaluated. For activated layers resulting from the gas-atomized NiAl50 precursor powder, a mean crystallite size of 7.8 nm was determined, whereas for layers originating from mixed Ni-Al/Mo and Ni-Al-Mo alloy, powder crystallite sizes of 6.5 and 3.5 nm, respectively, were calculated. According to Khaidar et al. (Ref 19), who developed an approximately linear relationship between the reciprocal value of the crystallite size and the effective surface area, such a reduction of the crystallite size leads to a near doubling of the effective surface area compared to that of commercial Ni-Al alloy. This effect should influence the electrochemical performance and result in a reduced electrochemical overvoltage.

3.2 *Raney Nickel/Co_3O_4 Matrix Composite Anodes*

Matrix composite layers consisting of Raney nickel and oxide electrocatalysts such as Co_3O_4 spinel were developed for anodic oxygen evolution in alkaline water electrolysis. Oxides of spinel or perovskite structure provide high catalytic activity; a Raney nickel matrix provides improved electrical conductivity and specific surface area.

Because oxide electrocatalysts exhibit a strong tendency for oxygen loss and decomposition at elevated temperatures, it has been difficult to process them to undecomposed, well-bonded, stable electrode layers. In applying conventional VPS parameters, Co_3O_4 is always reduced to CoO or metallic cobalt. Whereas parameters such as tank pressure or torch power are of minor influence, there is a strong dependence on plasma gas composition. As shown in Fig. 11, the use of only argon as plasma gas leads to strong decomposition to CoO; layer quality and deposition efficiency prove to be poor. In order to improve

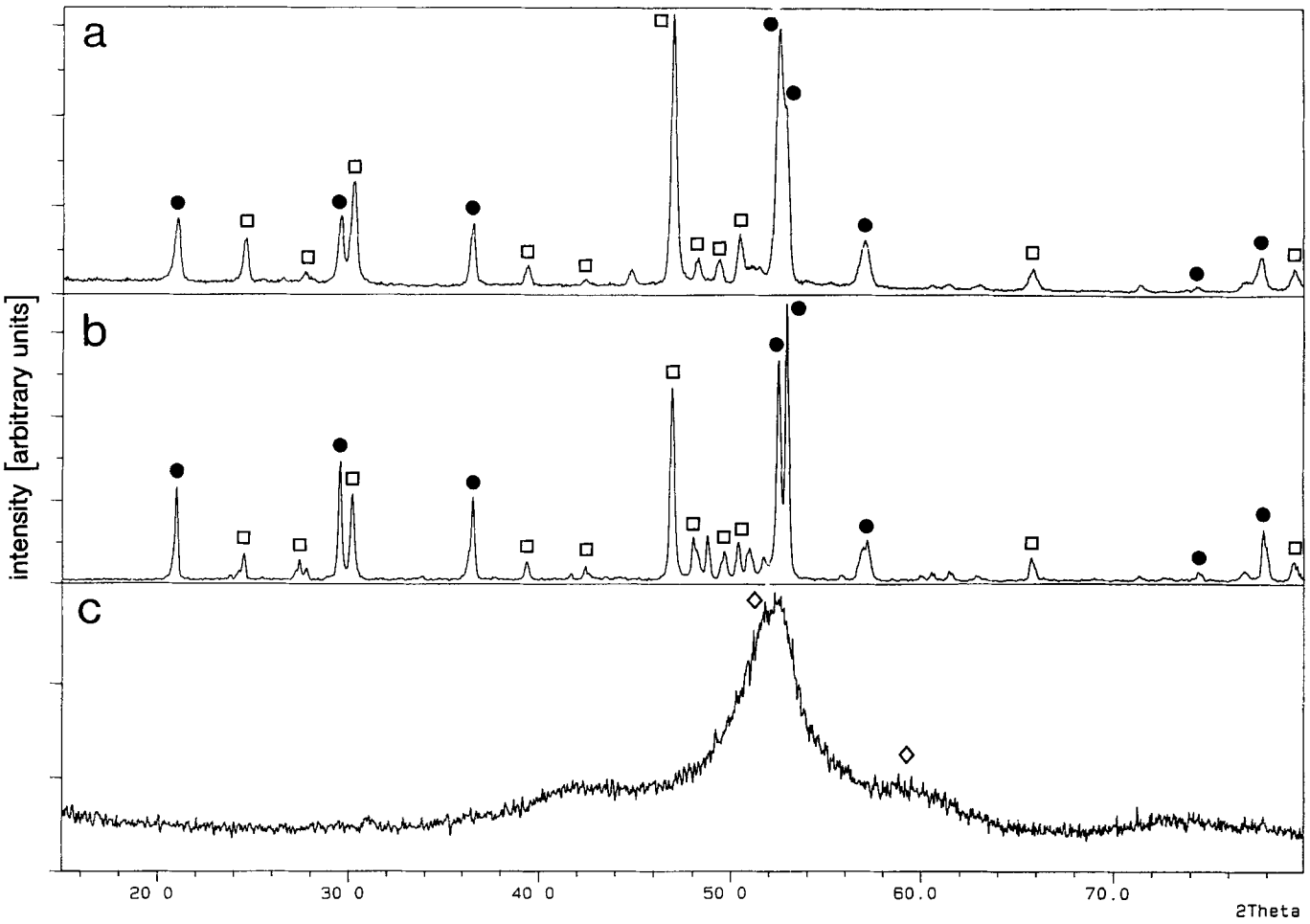

Fig. 9 XRD patterns of (a) Ni-Al-Mo alloy powder, (b) an as-sprayed VPS layer of Ni-Al-Mo alloy, and (c) the resulting activated layer. The crystallographic phases are indicated by the following symbols: ●, Ni_2Al_3, ❑ unknown phase, ◊ Ni.

both properties, helium, nitrogen, or hydrogen is usually added to the primary plasma gas, argon. These additives increase heat transfer to the powder particles, raise the plasma jet enthalpy, and extend the hot range of the jet, resulting in improved melting conditions of the spray powder. The layer stability and deposition efficiency can be improved with the addition of helium or nitrogen, but the decomposition to CoO remains unchanged. A considerable increase in deposition efficiency can be achieved with the addition of hydrogen, but a nearly total reduction of Co_3O_4 to metallic cobalt is observed in this case (Fig. 11e).

The fundamental strategy for overcoming decomposition and oxygen loss with VPS of thermally sensitive oxides is the inclusion of plasma-chemical effects by offering oxygen within the plasma jet. The arrangement of the injection ports along the Laval nozzle allows the feeding of additive gases into the plasma. Oxygen can be added to the powder carrier gas, argon, or it can be used exclusively as powder carrier gas, guaranteeing an additional intimate interaction with the feedstock. The injected molecular oxygen is dissociated and even ionized in the hot plasma zone, and therefore it is extremely effective in shifting the equilibrium between Co_3O_4 and CoO toward the oxygen-richer Co_3O_4 side. The application of powder carrier gas predominantly consisting of oxygen results in the desired reduction of Co_3O_4 decomposition, which is strongly dependent on the amount of oxygen, as expected. As shown by the XRD patterns in Fig. 12, where argon and helium were used as plasma gas, nearly undecomposed Co_3O_4 layers can be obtained by VPS if the oxygen feed exceeds 20% of the total gas flux involved in the plasma spray process. Decomposition of Co_3O_4 can also be suppressed considerably with argon and nitrogen as primary plasma gas (Fig. 12e), but deposition efficiency is lower using nitrogen instead of helium.

The parameters for spraying of Ni-Al/Co_3O_4 matrix coatings are given in Table 3. A cross section of a Ni-Al/Co_3O_4 anode layer is shown in Fig. 13. Ni-Al forms a matrix layer wherein Co_3O_4 electrocatalyst is embedded homogeneously, as confirmed by EDX analysis. There is no evidence by XRD that the intermetallic Ni-Al phases are affected seriously by the oxygen that is necessary to prevent Co_3O_4 decomposition. After activation a high-surface-area Raney nickel layer forms with a homogeneous distribution of cobalt, as shown by SEM/EDX studies.

3.3 *Electrochemical Performance*

The catalytic activity of the Raney nickel (Mo) cathodes and the Raney nickel/Co_3O_4 anodes was studied by obtaining IR-free polarization curves. The results for hydrogen evolution in 25 wt% KOH solution and 70 °C are summarized in Fig. 14, re-

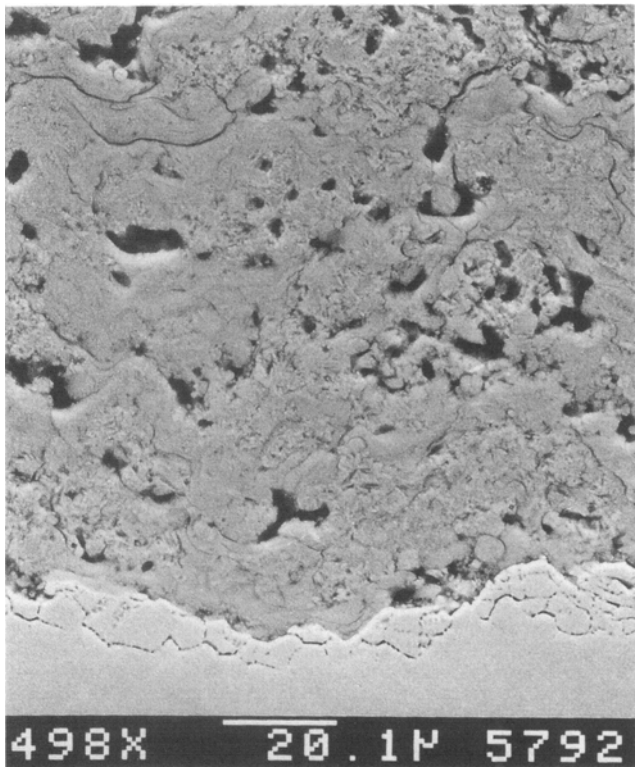

Fig. 10 Micrograph of a cross section of an activated Raney nickel (Mo) layer originating from Ni-Al-Mo precursor alloy

Table 3 VPS parameters for spraying of Ni-Al/Co_3O_4 mixed powder

Parameter	Value
Torch power	18 kW (360 A, 50 V)
Primary gas	Ar, 42 SLPM
Secondary gas	He, 50 SLPM
Powder feed gas	O_2, 20 SLPM
Tank pressure	50 mbar
Spraying distance	25 cm

SLPM ≡ standard liters per minute

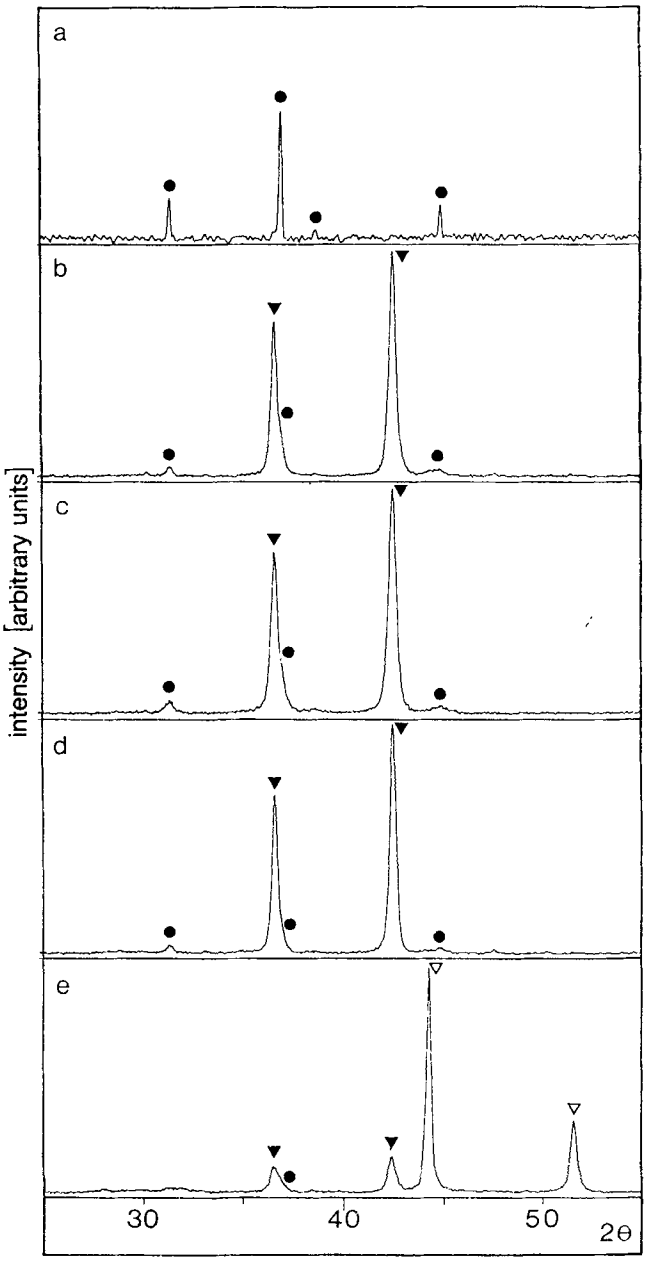

Fig. 11 XRD patterns of (a) Co_3O_4 powder and (b to e) as-sprayed VPS layers under various plasma gas compositions. (b) Ar. (c) Ar/He. (d) Ar/N_2. (e) Ar/H_2. The crystallographic phases are indicated by the following symbols: ● Co_3O_4, ▼ CoO, ∇ Co.

ferred to the hydrogen overvoltage of an uncoated perforated nickel sheet. With coatings from gas-atomized NiAl50, the hydrogen overvoltage at 1 A · cm^{-2} current density is in the range of 120 to 140 mV. The addition of molybdenum to the spray powder led to a decrease of overvoltage to between 80 and 100 mV, the best results being achieved with a molybdenum content of 5 wt%. The activated cathodes formed from Ni-Al/Mo precursor alloy show hydrogen overvoltage of 70 mV at a current density of 1 A · cm^{-2}. The Tafel slopes determined in the current density range of 0.25 to 1 A · cm^{-2} are reduced from 110 mV/decade for Raney nickel cathodes originating from Ni-Al precursor alloy to 70 mV/decade for those from mixed Ni-Al-Mo powder and 44 mV/decade for VPS cathodes resulting from ternary Ni-Al-Mo precursor alloy.

The polarization curve for oxygen evolution of Raney nickel/Co_3O_4 matrix anodes is shown in Fig. 15. The oxygen overvoltage at a current density of 1 A · cm^{-2} and 70 °C is in the range of 250 mV, which means a reduction of overvoltage of approximately 150 mV more than that achieved by an uncoated nickel sheet. The Tafel slope determined in the current density range of 0.25 to 1 A · cm^{-2} is 82 mV/decade.

The operation of VPS cathodes and anodes in electrolyzers proved a total reduction of the cell voltage at a current density of 0.3 A · cm^{-2} from 2.0 to 1.6 V, and mechanical and electrochemical behavior remained stable during long-term tests using constant and intermittent power supply for more than 10,000 h.

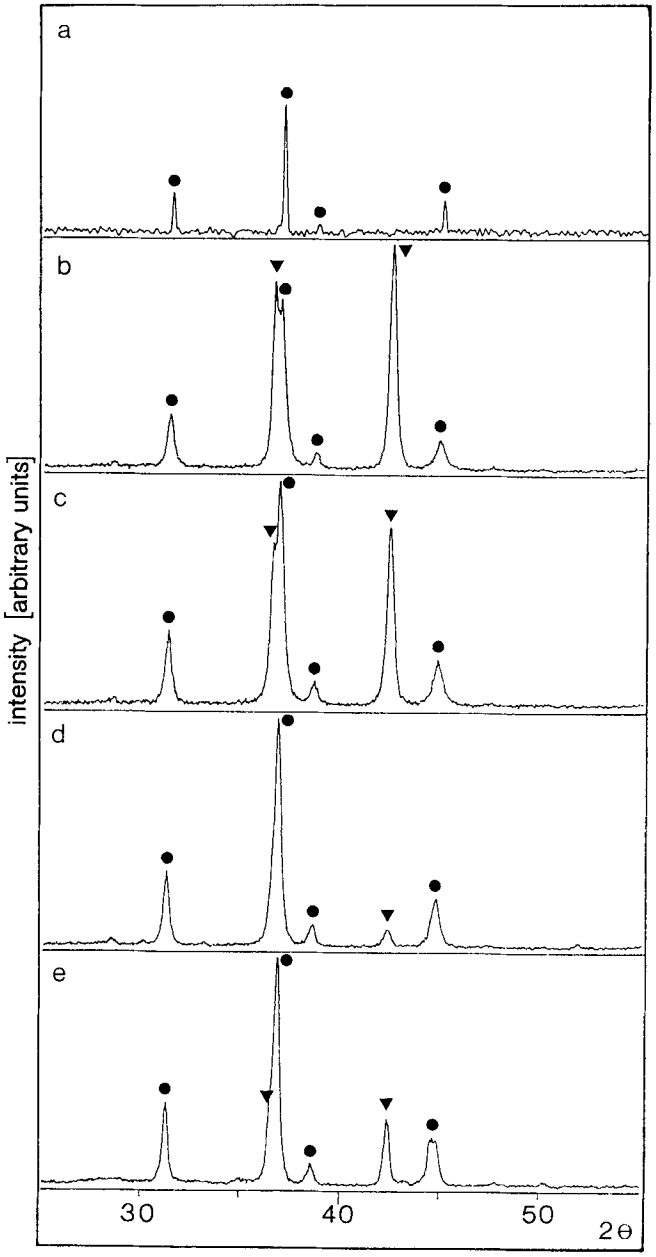

Fig. 12 XRD patterns of (a) Co_3O_4 powder and (b to e) as-sprayed VPS layers with different plasma gas (P) and powder carrier gas (C) compositions according to the following conditions: (b) P: Ar/He, C: Ar/O_2 (2/12 SLPM). (c) P: Ar/He, C: Ar/O_2 (2/15 SLPM). (d) P: Ar/He, C: Ar/O_2 (2/20 SLPM). (e) P: Ar/N_2, C: Ar/O_2 (2/10 SLPM). The crystallographic phases are indicated by the following symbols: ● Co_3O_4, ▼ CoO. SLPM ≡ standard liters per minute

4. Conclusions

It was demonstrated that high-performance electrodes for alkaline water electrolysis can be produced by means of VPS. Further work now has to be done to scale up the electrode manufacture by VPS. The next step, which is currently underway, is the production of electrodes with an area of 600 cm^2 to be tested in a 10 kW electrolyzer. Long-term investigations, especially under the conditions of intermittent operation by supplying the electrolyzer with current from solar energy, will be

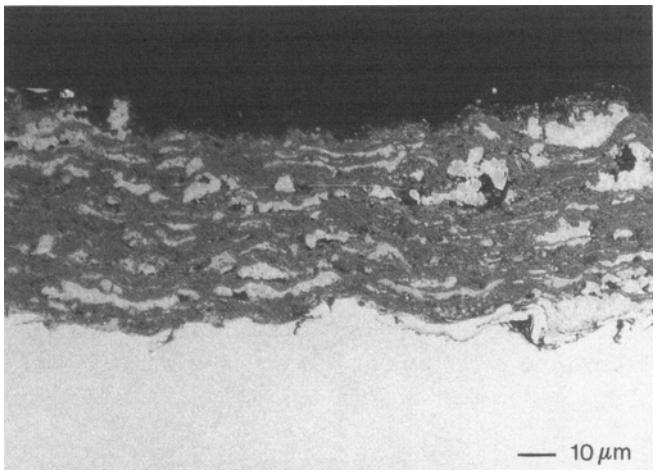

Fig. 13 Micrograph of a cross section of a Ni-Al/Co_3O_4 matrix composite layer. The dark phase represents the Ni-Al matrix in which the light Co_3O_4 phase is embedded.

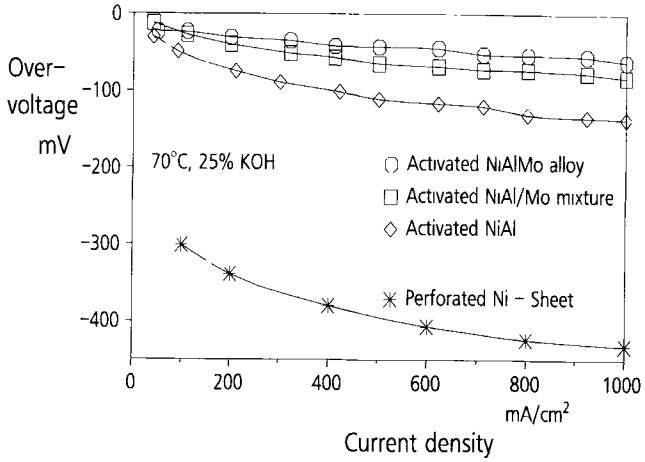

Fig. 14 Polarization curves of VPS Raney nickel cathodes resulting from different precursor alloys compared to the curve for uncoated perforated nickel sheet

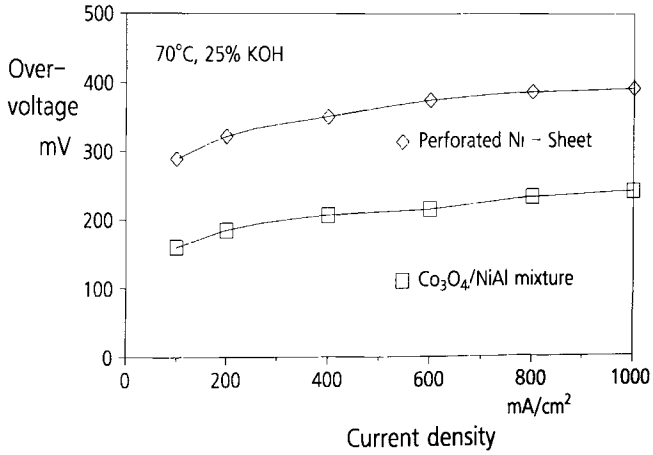

Fig. 15 Polarization curves of VPS Raney nickel/Co_3O_4 matrix composite anode compared to the curve for uncoated perforated nickel sheet

carried out to prove the high electrochemical performance and the suitability of VPS electrodes for intermittent operation on a technical scale.

The development of reactive plasma spraying that allows the processing of thermally sensitive oxides by VPS is not restricted to electrocatalysts for water electrolysis. The possibility of preventing oxygen loss and decomposition during plasma spraying by involving plasma-chemical effects is of eminent importance for many other oxides, such as those used for high-temperature superconductors and solid oxide fuel cells.

References

1. C.-J. Winter and J. Nitsch, Ed., *Hydrogen as an Energy Carrier*, Springer, 1988
2. E. Justi, W. Scheibe, and A. Winsel, "Doppelskellett-Katalysator-Elektrode," German Patent DBP 1,019,361, 1954
3. H. Wendt and V. Plzak, *Electrochemical Hydrogen Technologies*, Elsevier, 1989
4. D.E. Hall, Alkaline Water Electrolysis Anode Materials, *J. Electrochem. Soc.*, Vol 132 (No. 2), 1985, p 41C-48C
5. D.E. Brown, M.N. Mahmood, M.C.M. Man, and A.K. Turner, Preparation and Characterization of Low Overvoltage Transition Metal Alloy Electrocatalyst for Hydrogen Evolution in Alkaline Solutions, *Electrochim. Acta*, Vol 29, 1984, p 1551-1556
6. J. Divisek, H. Schmitz, and J. Balej, Ni and Mo Coatings as Hydrogen Cathodes, *J. Appl. Electrochem.*, Vol 19, 1989, p 519-530
7. S. Trasatti, Ed., *Electrodes of Conductive Metallic Oxides*, Elsevier, 1980
8. J. Balej, Electrocatalysts for Oxygen Evolution in Advanced Alkaline Water Electrolysis, *Int. J. Hydrogen Energy*, Vol 10 (No. 2), 1985, p 89-99
9. R. Henne, M.v. Bradke, W. Schnurnberger, and W. Weber, Development and Manufacture of Electrolyzer Components Applying Plasma Spraying under Reduced Pressure, *Advances in Thermal Spraying*, Pergamon Press, 1986
10. G. Schiller and V. Borck, Vacuum Plasma Sprayed Electrodes for Advanced Alkaline Water Electrolysis, *Int. J. Hydrogen Energy*, Vol 17 (No. 4), 1992, p 261-273
11. R. Henne, G. Schiller, W. Schnurnberger, and W. Weber, Role of Process Gas Composition at Vacuum Plasma Spraying of Oxide Electrocatalysts, *Proceedings of the Ninth International Symposium on Plasma Chemistry*, R. D'Agostino, Ed., 1989
12. W Mayr and R. Henne, Investigation of a VPS Burner with Laval Nozzle Using an Automated Laser Doppler Measuring System, *Proceedings of the First Plasmatechnik-Symposium*, H. Eschnauer, P. Huber, A.R. Nicoll, and S. Sandmeier, Ed., Vol 1, 1988
13. R. Henne, W. Mayr, and A. Reusch, Influence of Nozzle Geometry on Particle Behaviour and Coating Quality in High-Velocity VPS, *DVS-Berichte*, Vol 152, DVS-Verlag, Düsseldorf, 1993 (in German)
14. R. Henne, *J. Thermal Spray Technol.*, to be published
15. V.Y. Markiv, V.V. Burnashova, L.I. Pryakhina, and K.P. Myasnikova, Phase Equilibria in the Mo-Ni-Al System, *Izv. Akad. Nauk SSSR, Russ. Met.*, Vol 5, 1969, p 180-185
16. S. Kumar, Ternary Intermetallics in Aluminum, *Int. Mat. Rev.*, Vol 35 (No. 6), 1990, p 310-326
17. S. Hamar-Thibault and J. Masson, Nickel Divided Catalysts in the NiMo System: Correlation between Parent Alloy Catalyst, *J. Chim. Phys.*, Vol 88, 1991, p 219-232
18. M. Khaidar, C. Allibert, and J. Driole, Composition, Structure and Crystallite Size of Raney Catalysts Proceeding from Several Ni-Al and Fe-Al Intermetallic Phases, *Mat. Res. Bull.*, Vol 17, 1982, p 329-337